MODIFIED PHOTOIMAGEABLE THICK-FILM PROCESS FOR MILLIMETER-WAVE RECTANGULAR WAVEGUIDE APPLICATIONS

M. Daigle[*], T. Djerafi, and K. Wu

Département de génie électrique, Centre de recherche PolyGrammes, École Polytechnique de Montréal, Montréal, Canada

Abstract—This paper presents the design and fabrication of a class of dielectric filled rectangular waveguides using a multilayer photoimageable thick-film technique. The original fabrication technique is modified to shorten fabrication time and improve waveguide thickness to reduce transmission structure losses. The materials used are first characterized before the wave-guiding properties are extracted. The fabricated waveguides show excellent results in term of loss and a 1% variation in permittivity over a wide frequency range of 10–100 GHz. To demonstrate the practical applications of this modified fabrication technique, 5th and 3rd order band-pass filters are designed and fabricated. The different incertitude on the fabrication issues is studied showing an effect on the bandwidth and central frequency. The measurement results of the fabricated prototypes agree well with the simulated ones. A broadband 3 dB coupler is designed and fabricated covering both V and W bands. The measurements results for this circuit show good performance with 23% of bandwidth and are in good agreement with the simulations.

1. INTRODUCTION

In recent years, millimeter wave technologies and the related fabrication techniques have attracted significant interest from the academia and industry due to several reasons. Firstly, the increased absolute bandwidth provided by a higher frequency operation allows for much larger transfer rates in telecommunication [1]. Secondly, the important atmospheric absorption losses at certain frequencies

(60 GHz, for example) provide privacy and frequency reusability for small scale or micro-cellular wireless networks [2]. Finally, shorter wavelengths permit imagery applications in various fields from aircraft imaging assistance for low visibility conditions to security applications [3, 4]. Until recently, only the traditional machined rectangular waveguides and planar technologies (microstrip, coplanar waveguides, etc.) have been used to fabricate commercially available millimeter wave components, circuits and systems. Metallic rectangular waveguides provide unparalleled circuit qualities (high Q factor, extremely low losses), but they are increasingly costly and difficult to fabricate as frequencies go up and cannot be mass produced. They also tend to be bulky and heavy. The reverse is true for planar circuits, while they are inexpensive, easy to mass-produce and very compact, they exhibit much higher losses, especially at high frequencies.

Substrate integrated waveguides (SIW) have been proposed as a vital solution to these problems [5–7]. These SIW circuits synthesize rectangular waveguides with metalized vias or slots drilled into the substrate. For the fabrication of millimeter-wave circuits, the SIW constitutes a compromise between the quality of rectangular waveguides and the ease of fabrication of planar circuits. However, the SIW circuits can hardly be mass-produced because of the laser drilling needed in their fabrication. In addition, a higher frequency design over the millimeter-wave frequency range and beyond will demand more and more fabrication precision. For this reason, the photoimageable thick film waveguides have been proposed by Aftanasar et al. [8] and they were further developed in [9] and [10].

In this work, dielectric filled rectangular waveguides fabricated with a photoimageable thick film process are presented which exhibit all the advantages of SIW structures while allowing mass production and demanding less costly installations. The fabrication technique was also improved to provide a shorter fabrication time and an increased waveguide thickness. Material and process characterization is presented together with application examples including filters and a 3 dB coupler.

2. PHOTOIMAGEABLE THICK FILM PROCESS

The photoimageable thick film process was developed to improve the resolution of existing screen printing technologies. Instead of using the screen to pattern the dielectric and metal pastes, a photosensible compound is added to the paste. Upon exposure to UV light, the paste hardens and only the unexposed parts will dissolve in the development
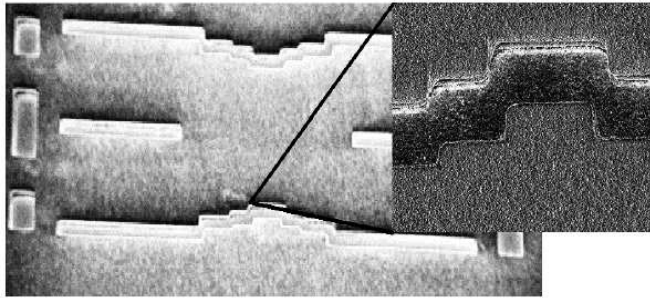
Figure 1. Scanning Electron Microscope (SEM) image of the presented coupler before trenches metallization. The trench is 200 μm wide and 100 μm deep. Fine detail zooming shows the slightly rounded corners and alignment tolerance of the process.
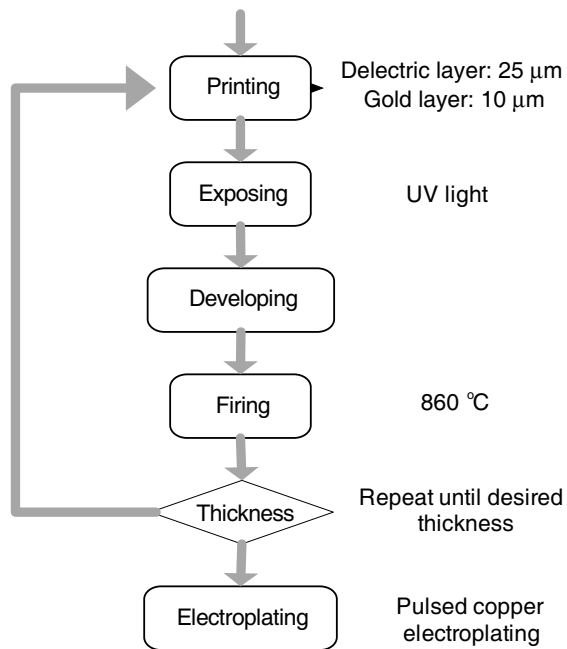

Figure 2. Process flow for the fabrication of metallic waveguide with photoimageable process. Electroplating is performed as the last step to fill the sidewalls with copper. The first sequence is repeated until the desired thickness is obtained.

solution. Once developed, the paste is fired at high temperature. This process is repeated for each layer of dielectric and metallic paste needed. Minimum feature size is under 20 µm, which is amply sufficient for most millimeter-wave waveguide applications.

   With the proposed modified method, the metallic trenches that constitute the sidewalls of the waveguides are plated using a pulsed copper electroplating once all the dielectric layers are fired, as can be seen on Figure 1. This allows for a rapid filling of the trenches whereas eight layers are necessary in [10]. Considering that each layer necessitates a full day of processing (principally caused by firing and cooling time), this improvement can considerably reduce the fabrication time. Figure 2 resumes the process used for the metallic waveguide fabrication. In this work, all waveguides are fabricated using four dielectric layers, which give a total 100 µm thickness. Adding more layers would reduce losses but also augment fabrication time. Electroplating is performed using a current source providing both positive and negative current pulses. This technique increases plating uniformity and prevents copper spiking which often appears in the pattern corners or edges. Once the sidewall trenches are fully metalized, the final metal layer is applied using the photoimageable gold paste. If very fine patterns are needed for the top metal (high frequency slot antennas, EBG structure, etc.), sputtered metal and standard photolithography can replace the photoimageable paste.

3. MATERIAL AND WAVEGUIDE CHARACTERIZATION

The photoimageable pastes used are produced by DuPont$^{\text{TM}}$ under the commercial name of Fodel®; product number is QM44F for dielectric paste and 5989 for gold paste. Since these products were not originally intended for high frequency applications, the dielectric constant has to be determined with sufficient precision before the circuit design can be done. The circuits fabricated for material characterization are shown in Figure 3. The dielectric constant is measured using several microstrip ring resonators with different radius as explained in [11]. To extract the permittivity ε_r, the following four equations are necessary:

$$\varepsilon_{eff}(f) = \left(\frac{nc}{2\pi r f_0}\right)^2 \tag{1}$$

$$\varepsilon_r = \left(\frac{2\varepsilon_{eff} + M - 1}{M + 1}\right) \tag{2}$$
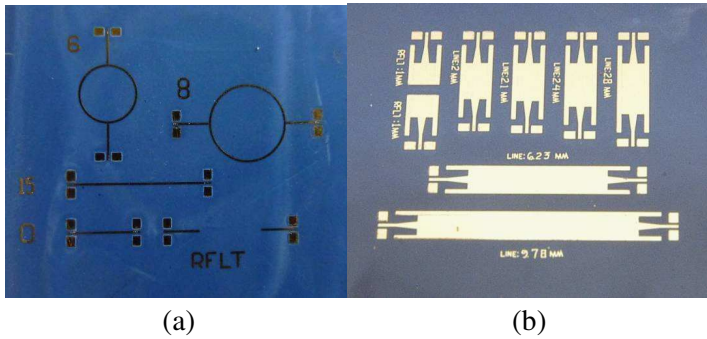
(a)   (b)

Figure 3. Fabricated circuits for material characterization. (a) Ring resonators for dielectric constant measurements. (b) Different waveguide lengths and a TRL calibration kit for total loss measurements.
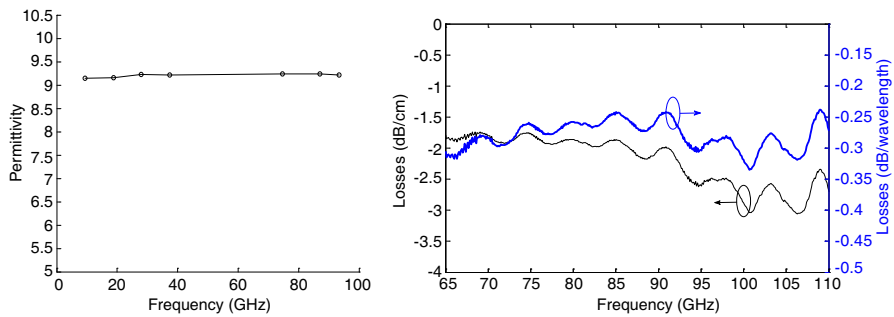

Figure 4. Measured dielectric constant of Fodel® QM44F paste and total measured losses of the fabricated rectangular waveguides.

$$M = \left(1 + \frac{12h}{W_{eff}}\right)^{-\frac{1}{2}} \tag{3}$$

$$W_{eff} = W + \left(1.25\frac{t}{\pi}\right)\left(1 + \ln\left(\frac{2h}{t}\right)\right) \tag{4}$$

where n is the number of half wavelengths, c is the speed of light, f_0 is the resonant frequency, W the width of the microstrip, h the thickness of the dielectric, r the mean radius of the resonator and t the metal thickness. Results are presented in Figure 4 and show a surprisingly small variation of 1% over the entire measured band, from 10 to 100 GHz.

Using this information, a number of rectangular waveguides are

fabricated with a width of 1.04 mm, giving a cut-off frequency of 50 GHz. Using different waveguide lengths and a TRL calibration kit fabricated on substrate to de-embed the transitions effects, the total loss of the fabricated waveguides is shown in Figure 4. Total losses are under 3 dB/cm, or 0.34 dB/wavelength up to 110 GHz, and less than 2 dB/cm from 65 to 90 GHz. The observed ripples are supposedly caused by the imperfect calibration. For all the measurements performed in this paper, a Suss MicroTec automated probing station with 250 μm pitch ground-signal-ground probes is used in conjunction with an Anritsu 37397C vector network analyzer equipped with WR-10 modules for the 65–110 GHz band. These results are very encouraging and compare advantageously with the standard SIW circuits at these frequencies.

4. FILTER DESIGN AND RESULTS

To demonstrate the capabilities of this fabrication technique, one of the most ubiquitous and useful millimeter wave circuit elements is fabricated; the band-pass filters. Since the photoimageable technology produces true rectangular waveguides (as opposed to the synthesized waveguides as SIW), it is very simple to design such filters by directly using the well-known equations for traditional metallic waveguides. The design techniques involve impedance inverters to represent the filter coupling section [12]. The inductive metal planes can be modeled as parallel inductive shunts connected between transmission lines of various electrical lengths. The inductive irises are approximated using empirical results from Marcuvitz [13].

Third and fifth order Chebychev iris bandpass filters centered at 80 GHz and 75 GHz respectively are designed to be incorporated onto diplexer. The layout of the third order filter centered at 80 GHz is presented in Figure 5 with all the design dimensions. The effect of the
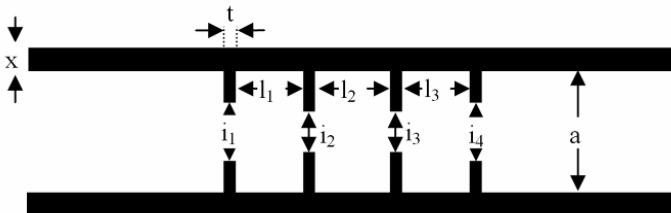

Figure 5. Layout and dimensions for the third order band-pass filter centered at 80 GHz.

Table 1. Third order filter at 80 GHz parameters.

Variable	Value (mm)	Variable	Value (mm)
i_1	0.500	l_1	0.590
i_2	0.346	l_2	0.653
i_3	0.346	l_3	0.590
i_4	0.500		

Table 2. Fifth order filter at 75 GHz parameters.

Variable	Value (mm)	Variable	Value (mm)
i_1, i_6	0.636	l_1	0.601
i_2, i_5	0.461	l_2	0.704
i_3, i_4	0.407	l_3	0.727
l_4	0.704	l_5	0.601

iris thickness is not considered to define the initial parameters. The HFSS software is used to optimize these parameters considering the effect of the iris thickness. For ease of fabrication, the iris thickness t is fixed at 100 μm and the sidewall thickness x is 200 μm. The optimized design dimensions are tabulated in Tables 1 and 2.

As shown in the close-up view in Figure 1, due to the fabrication process, the corners are slightly rounded. This effect and the thickness of the iris are the most critical parameters in the fabrication process. To estimate the potential consequence of these parameters, the simulated result are showed in Figure 6. The 25 μm variation on the iris thickness as illustrated in Figure 7(a) causes a frequency shift of 1.75 GHz and modifies the bandwidth of the filter. As shown in Figure 6(b), the round corner effect causes a downward shift of the first stop frequency. From the perfectly sharp corner to the 50 μm rounded corner, this shift is about 2 GHz. The second stop frequency is less affected. The rounded edges effectively enlarge the resonant cavities, lowering central frequency and making the cavities more oval shaped which consequently widen the pass band [14]. This rounding can be dissymmetric, Figure 6(c) show a variation of one corner when the other one is fixed to 50 μm, the effect seems to saturate. All this incertitude causes more attenuation at either frequencies.

The photographs of the filters are shown in Figure 7. Measured and simulated results are presented in Figure 8. The measured insertion loss is 3.74 dB and the return loss is less than 16.7 dB in
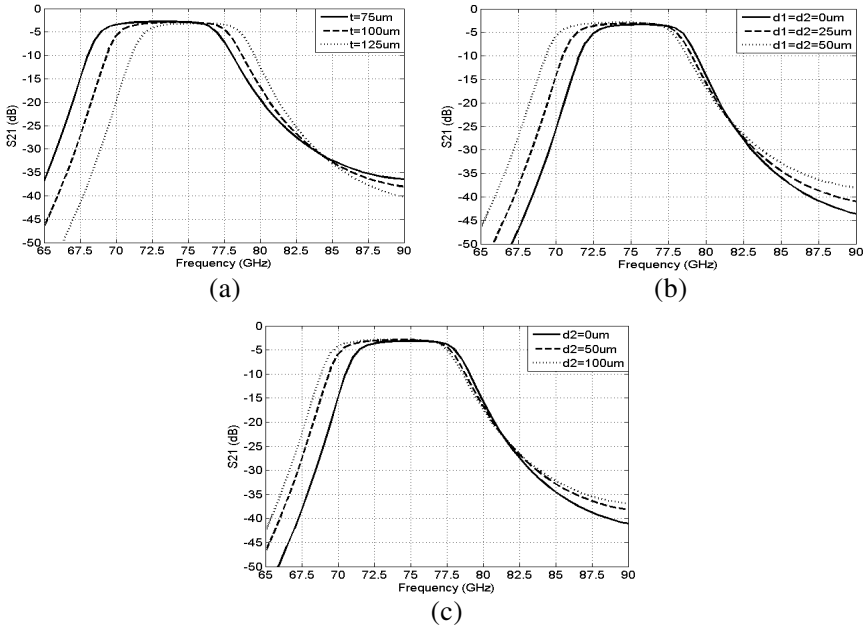
Figure 6. Simulations of fabrication tolerance effects: (a) the effect of iris thickness, (b) the effect of the rounded corner, (c) effect of the dissymmetric rounded corner.
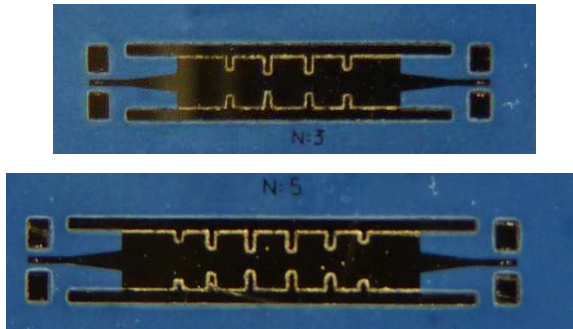

Figure 7. Fabricated Filter: the third order iris band-pass filter centered at 80 GHz, and the fifth order iris band-pass filter centered at 75 GHz.
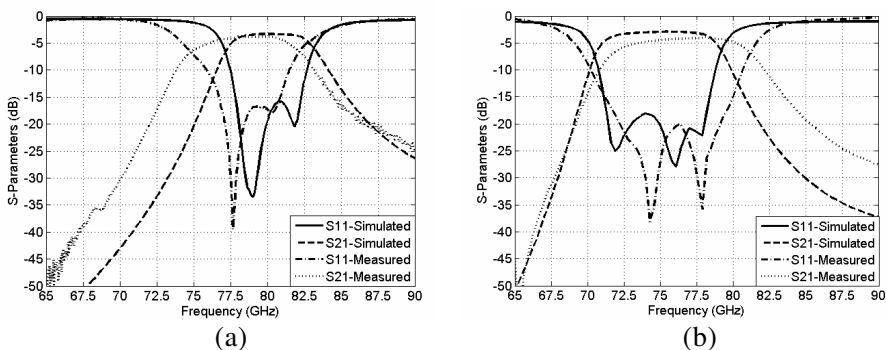
Figure 8. Simulated and measured results of: (a) the third order iris band pass filter centered at 80 GHz, (b) the fifth order iris band pass filter centered at 75 GHz.
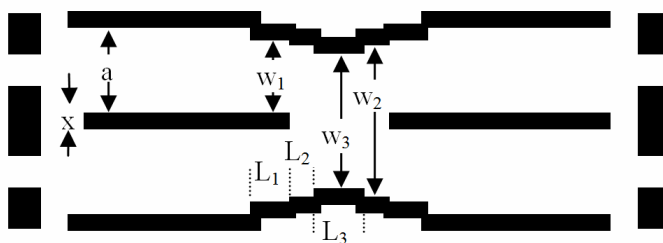

Figure 9. Layout and dimensions of the 3 dB coupler.

the pass-band. The measured bandwidth is slightly widened and the central frequency is shifted from 80 GHz to 78 GHz. This effect is due to the rounded iris edges and variation of the iris thickness as discussed above. The fifth order filter shows similar performance with more loss caused by the additional length.

5. COUPLER DESIGN AND RESULTS

To further demonstrate the capabilities of the photoimageable thick film process in millimeter wave applications, a broadband 3 dB coupler is implemented. Short-slot Riblet coupler [15], with three H-plane impedance steps is designed. These impedance steps are used to prevent the undesired TE_{30} mode from propagating [16].

In this design, the coupling section consists of one continuous

aperture L $(L_3 + 2L_2)$ as shown in Figure 9. The phase difference between the two modes is:

$$\varphi = 2\pi \left(\frac{l_3}{\lambda_{ge}} - \frac{l_3}{\lambda_{go}} \right) \qquad (5)$$

λ_{ge} and λ_{go} are the even and odd mode wavelengths in the substrate integrated waveguide. In the standard SIW technology, this coupler was studied in [17], a relative bandwidth of 12% was achieved with a limited isolation. Waveguide steps were used to improve the input matching in [18], resulting in a 20% bandwidth.

The coupler is designed using full wave simulator *HFSS* for frequency operation between 67 and 85 GHz, giving it a simulated bandwidth of 23%. A complete layout of the coupler design is presented in Figure 9 and the parameters are tabulated in Table 3.

Table 3. Broad-wall directional coupler parameters.

Variable	Value (mm)	Variable	Value (mm)
a	1.021	x	0.200
w_1	0.899	L_1	0.496
w_2	1.827	L_2	0.313
w_3	1.637	L_3	0.634

Since the measurement setup only allows two-port measurements, 3 identical couplers are fabricated, each with two fully metalized ports and two ports metalized with only 50 nm of titanium as presented in [19]. Back reflections are caused by a variation of impedance and the impedance is solely defined by the geometric change. Since no impedance step is observed at the gold/titanium interface, there will be no back refection at this interface. The full reflection will however happen at the circuit end. Measurements of such a titanium port showed that S_{21} parameter reduced by 45 dB due to resistive losses whereas S_{11} remains unaffected. In consequence, the reflected power into the coupler will be attenuated by more than 90 dB, which is more than enough for this measurement. A photograph of the couplers with the titanium ports as well as a schematic representation of the measurement setup is presented in Figure 10.

The results obtained are presented in Figure 11. The agreement with the simulation is quite good. The return loss is less than 20 dB in the bandwidth and beyond from 69 to 90 GHz. Results for the isolation are not as good as expected; it is less than 15 dB in the bandwidth. This can be explained by a very small distance between
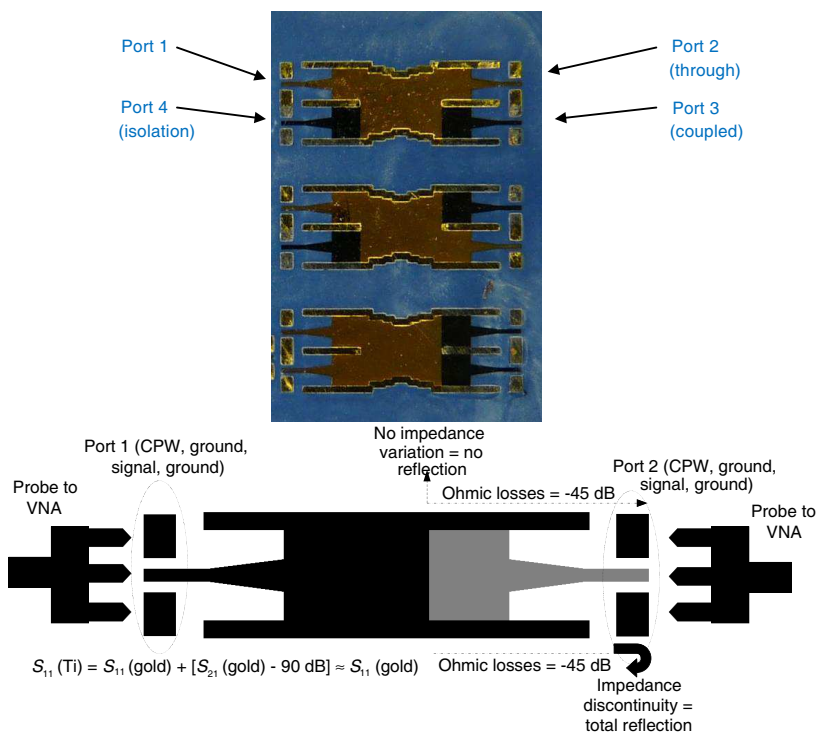
Figure 10. Fabricated 3 dB couplers with resistive titanium ports for measurements. From the top to bottom, the three couplers are configured for the measurement of through port (S_{12}), coupled port (S_{13}) and isolation (S_{14}).
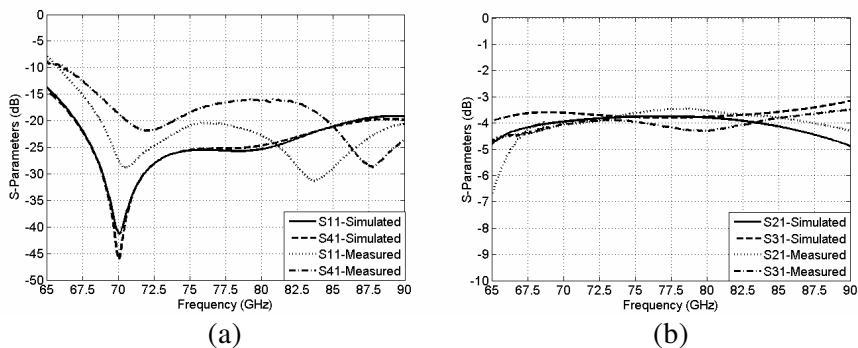

Figure 11. Simulated and measured results for the 3 dB coupler: (a) matching (S_{11}) and isolation (S_{41}), (b) coupling coefficient (through port (S_{21}) and coupled port (S_{31})).
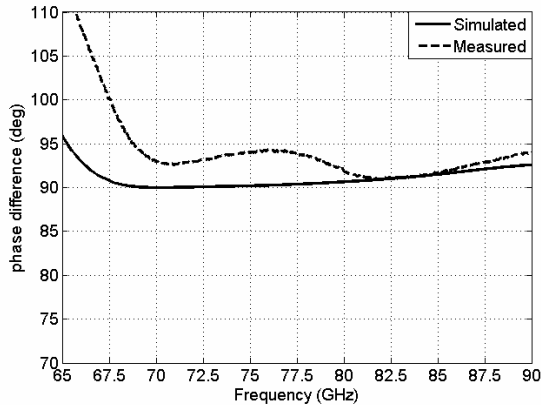
Figure 12. Phase difference between through and coupled ports.

the two probes in the test setup. Both probes are only separated by less than 1 mm and a coupling is probably the cause of the higher than expected isolation. Total loss of the coupler is measured around 1 dB and the imbalance between the through and coupled port is less than ±0.5 dB. Phase difference is maintained close to 90° in the operating band. The results obtained are presented in Figures 11 and 12.

6. CONCLUSION

In this work, a class of dielectric filled rectangular waveguides fabricated with a photoimageable thick film process are presented which exhibit all the advantages of SIW while allowing a mass production and demanding less costly installations. The cylindrical or rectangular holes which are needed in the fabrication of the standard SIW are avoided and the photoimageable technology produces true rectangular waveguides. The material used is characterized to find out the equivalent permittivity and loss. The material and fabrication process show an excellent stability form 10 to 100 GHz. Filters of the third and fifth orders are designed. The critical parameters are studied to estimate the fabrication tolerance. The measured results agree well with the estimated ones. The process is used to build a 3 dB hybrid coupler. To measure the four port device, a resistive attenuator on titanium is proposed and realized. The measured coupler performance has shown a bandwidth of almost 25%. The process can be used to build more complex junctions and many other integrated circuits such as N-port power divider, multiplexer or beamforming network up to the terahertz frequency range.

REFERENCES

1. Razavi, B., "A 60-GHz CMOS receiver front-end," *IEEE J. Solid-State Circuits*, Vol. 41, No. 1, 17–22, Jan. 2006.

2. Smulders, P., "Exploiting the 60 GHz band for local wireless multimedia access: Prospects and future directions," *IEEE Communications Magazine*, Vol. 40, No. 1, 140–147, 2002.

3. Martin, C., J. Lovgerg, S. Clark, and J. Galliano, "Real time passive millimeter-wave imaging from a helicopter platform," *Proceedings of the 19th Digital Avionics Systems Conferences*, Vol. 1, 2B1/1–2B1/8, 2000.

4. Essen, H., A. Wahlen, R. Sommer, W. Johannes, J. Wilcke, M. Schlechtweg, and A. Tessmann, "A versatile, miniaturized high performance W-band radar," *German Microwave Conference*, 1–4, 2009.

5. Wu, K., D. Deslandes, and Y. Cassivi, "The substrate integrated circuits — a new concept for high-frequency electronics and opto-electronics," *6th International Conference on Telecommunications in Modern Satellite, Cable and Broadcasting Service, 2003, TEL-SIKS 2003*, Vol. 1, P-III-P-X, 2003.

6. Deslandes, D., "Design equations for tapered microstrip-to-substrate integrated waveguide transitions," *IMS 2010*, 704–708. 2010.

7. Hirokawa, J. and M. Ando, "Single-layer waveguide consisting of posts for plane wave excitation in parallel plate," *IEEE Transactions on Microwave Theory and Techniques*, Vol. 46, No. 5, 625–630, May 1998.

8. Aftanasar, M. S., P. R. Young, I. D. Robertson, J. Minalgiene, and S. Lucyszyn, "Photoimageable thick-film millimetre-wave metal-pipe rectangular waveguides," *Electronic Letters*, Vol. 37, No. 18, 1122–1123, 2001.

9. Stephens, D., P. R. Young, and I. D. Robertson, "Millimeter-wave substrate integrated waveguides and filters in photoimageable thick-film technology," *IEEE Transactions on Microwave Theory and Techniques*, Vol. 53, No. 12, 3832–3838, 2005.

10. Henry, M., C. E. Free, B. S. Izqueirdo, J. Batchelor, and P. Young, "Millimeter wave substrate integrated waveguide antennas: Design and fabrication analysis," *IEEE Transactions on Advanced Packaging*, Vol. 32, No. 1, 93–100, 2009.

11. Samanta, K. K., D. Stephens, and I. D. Robertson, "Ultrawide-band characterisation of photoimageable thick film materials for microwave and millimeter-wave design," *IEEE MTT-S Int. Mi-*

crowave Symp., 2005.

12. Matthaei, G. L., L. Young, and E. M. T. Jones, *Microwave Filters, Impedance Matching Networks and Coupling Structure*, Artech House, Dedham, 1985.

13. Marcuvitz, N., *Waveguide Handbook*, McGraw-Hill, 1951.

14. Sammoura, F., Y.-K. Fuh, and L. Lin, "Micromachined plastic W-band bandpass filters," *Sensors and Actuators*, Vol. 147, 47–51, 2008.

15. Riblet, H. J., "The short-slot hybrid junction," *Proc. IRE*, Vol. 40, 180–184, Feb. 1952.

16. Hildebrand, L. T., "Results for a simple compact narrow-wall directional coupler," *IEEE Microwave and Guided Wave Letters*, Vol. 10, No. 6, 231–232, Jun. 2000.

17. Hao, Z. C., W. Hong, J. X. Chen, H. X. Zhou, and K. Wu, "Single-layer substrate integrated waveguide directional couplers," *IEE Proc. Microw. Antennas Propag.*, Vol. 153, No. 5, Oct. 2006.

18. Cassivi, Y., D. Deslandes, and K. Wu, "Substrate integrated waveguide directional couplers," *ASIA-Pacific Conf.*, Kyoto, 2002.

19. Djerafi, T., M. Daigle, H. Boutayeb, X. Zhang, and K. Wu, "Substrate integrated waveguide six-port broadband front-end circuit for millimeter-wave radio and radar systems," *European Microwave Conference*, 77–80, 2009.